Topology — *About "Bulky" Links, generated by Generalized Möbius Listing's bodies GML_3^n*, by I. Tavkhelidze, C. Cassisa, J. Gielis and P. E. Ricci, communicated on 9 November 2012.

Dedicated to the memory of Gaetano Fichera in recognition of his contributions to the Theory of Elasticity

Abstract. — In the present paper we consider the "bulky knots" and "bulky links", which appear after cutting a Generalized Möbius Listing's GML_3^n body (whose radial cross section is a plane 3-symmetric figure with three vertices) along different Generalized Möbius Listing's surfaces GML_2^n situated in it. This article is aimed to investigate the number and geometric structure of the independent objects appearing after such a cutting process of GML_3^n bodies. In most cases we are able to count the indices of the resulting mathematical objects according to the known tabulation for Knots and Links of small complexity.

Key words: Analytic representation, Möbius strip, Möbius-Listing's surfaces, Ribbon Knots, Links.

Mathematics Subject Classification: 53A05, 51B10, 57M25.

Premise

This article comes out from the desire to express, on the occasion of the 90th anniversary of his birth, a grateful memory to Professor Gaetano Fichera, a Master who opened the road for a scientific career to many of us.

Gaetano Fichera was one of the last universal mathematicians, who possesed a wide overview of the most important developments of a discipline which is entering more and more in every field of human activities.

Our first author, Ilia Tavkhelidze, was attracted to the study of very general surfaces and bodies—and their connections with the theory of knots and links—including as particular cases the initial investigations due to Möbius and Listing. Ilia's motivation started from a clever remark by his PhD advisor, the famous Russian mathematician Olga A. Oleinik, one of the most powerful pupils of Ivan G. Petrovskii. For a long time, Olga was linked to Prof. Fichera by scientific and friendly interests, so strongly that she was able to complete a posthumous work of Gaetano about a difficult problem of thermoelasticity. Olga observed that the solutions of boundary value problems for partial differential equations strongly depend on the geometrical properties of the domain in which the problem is considered. This was the initial motivation of Ilia's works dedicated to some geometric and structural properties of surfaces and bodies.

In these works Ilia subsequently attracted some former pupils of Fichera, in particular Caterina Cassisa and Paolo Emilio Ricci, and more recently Johan Gielis, who, starting from a different field of investigations, namely botany and biology, was able to derive a general formula unifying extremely different plane natural shapes appearing in natural bodies.

Very enlightening are Johan's introductions to some articles in collaboration [6], [7], emphasizing the importance of connections between pure geometrical investigations and natural phenomena. Without repeating here his considerations we want only to point out that surfaces and bodies generalizing Möbius and Listing's ones frequently appear in different fields of Natural Sciences, like botany, biology, neurology, etc. This is the main motivation even of the present work, which focusses on 3-symmetrical GML bodies. As one example, this symmetry is fundamental in the monocot group of flowering plants, which includes all grasses, orchids and flowers like tulips, irises and lilies.

INTRODUCTION

A tabulation of knots and links of small complexity (thread structure without interior geometry) can be found in several works (see e.g. [4], [9], [10], [11], [13], [20]). In previous articles [14], [15] a wide class of geometric figures "Generalized Twisting and Rotated" bodies—shortly GTR_m^n—(sometimes called "surfaces of Revolution" see e.g. [5], [8]) was defined through their analytic representations. In particular cases, the analytic representation gives back many classical objects (torus, helicoid, helix, Möbius strip,... etc.). This article is aimed to consider some geometric properties of a wide subclass of the above mentioned surfaces, by using their analytical representation. In this article we consider bulky knots and links which appear after a cutting process of Generalized Möbius—Listing's bodies GML_3^n along "parallel" lines of their "Ribs". In previous articles [3], [16], [17], [18], [19] a set of Generalized Möbius Listing's surfaces—shortly GML_m^n, which are a particular case of the GTR_m^n bodies, have been defined, and we considered the cases when the GML_m^n surface is affected by a "k-times cutting" along its basic line. But now, basing on our previous results, see e.g. [18], [19] we consider the case when GML_3^n is a body, whose radial cross section is given by a plane 3-symmetric convex figure with 3 vertices.

Five main question are examined in this article:

1. How many independent geometric objects appear after the cutting process?
2. What is the geometric structure of the objects which appear after the cutting process?
3. What are the indices, according to the classical tabulation of links (see e.g. [4], [9], [20],...), of the bulk link which appear after the cutting process?
4. What similarities and differences are between the cutting processes of GML_3^n-bodies and GML_3^n-surfaces?
5. What similarity and difference are between the cutting processes of GML_2^n and GML_3^n-bodies?

All possible variants, appearing after the cutting processes of GML_2^n-bodies, were studied in [7].

<div align="center">NOTATIONS</div>

In this article we use following notations:

- X, Y, Z, or x, y, z—is the ordinary notation for coordinates;
- τ, ψ, θ—are space values (local coordinates or parameters in parallelogram):

(1)
  1. $\tau \in [\tau_*, \tau^*]$, where $\tau_* \leq \tau^*$, are non-negative constants;
  2. $\psi \in [0, 2\pi]$;
  3. $\theta \in [0, 2\pi]$

- $P_m \equiv A_0 A_1 \ldots A_{m-1}$—denotes a "Plane convex figure with m-vertices", in particular P_m is a "m-symmetric polygon" or "regular polygon" and m is the number of its angles or vertices. In the general case the edges of "polygons" are not always straight lines ($A_i A_{i+1}$ could be, for example: arcs of circle or ellipse, edge of epicycloid, or part of Gielis's line [5], and so on); In this article we mainly consider P_3—"Plane convex 3-symmetric figure with 3-vertices". A simple example is shown in Fig. 1.b., and in Figures 1.a., 1.c., 1.d. we show photos of Haeckel's Diatomeas.

(2)
$$x = p(\tau, \psi), \quad z = q(\tau, \psi)$$

or

(2*)
$$x = p(\tau, \psi) \cos \psi, \quad z = p(\tau, \psi) \sin \psi$$

are the analytic representations of an "m-symmetric Plane figure" P_m, usually $p(0,0) = q(0,0) = 0$ and the point $(0,0)$ is the center of symmetry of this polygon (see e.g. [15] or [5]).

- For example—in this paper, without loss of generality, dealing with proofs relevant to a plane P_3-figure, we use the Gielis's super-formula and its simple variant

(3)
$$p(\tau, \psi) \equiv \left[\left| \frac{\cos\left(\frac{m_1 \psi}{4}\right)}{a} \right|^{n_2} + \left| \frac{\sin\left(\frac{m_2 \psi}{4}\right)}{b} \right|^{n_3} \right]^{-1/n_1},$$

with $\tau = 1$, $m_1 = m_2 = 3$, $a = b = 1$ and $n_1 = n_2 = n_3 = 1$ (see Fig. 1.b.);
- $PR_m \equiv A_0 A_1 \ldots A_{m-1} A_0' A_1' \ldots A_{m-1}'$ denotes an orthogonal prism, whose ends $A_0 A_1 \ldots A_{m-1}$ and $A_0' A_1' \ldots A_{m-1}'$ define P_m (see e.g. Fig. 2.a.)
- PR_∞—is an orthogonal cylinder, whose cross section is a circle, denoted by P_∞.
- $\tilde{x}$, $\tilde{z}$, θ—are space values (local coordinates or parameters in the cylinder ($\tau_* \equiv 0$) or in the pipe ($\tau_* > 0$) correspondingly)

(4) $$PR_\infty \equiv \{(\tilde{x} = \tau \cos \psi, \tilde{z} = \tau \sin \psi, \theta) : \tau \in [\tau_*, \tau^*]; \psi \in [0, 2\pi]; \theta \in [0, 2\pi]\}.$$
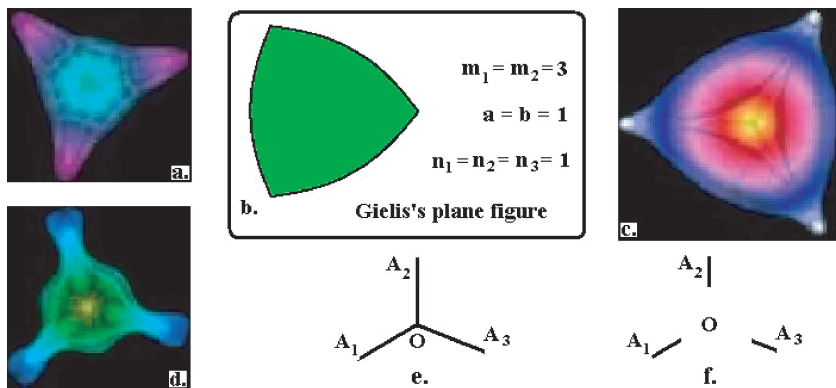
Figure 1

- $P_m^* \equiv OA_0A_1 \ldots A_{m-1}$—denotes a "Plane star-like figure with m-symmetry", in particular P_m^* is a "regular simple star" and m is the number of its wings or vertices. If $p(\tau, \psi)$ in formula (2^*) has the form

$$(2') \qquad p(\tau, \psi) \equiv \tau \sum_{i=0}^{m-1} l_i \cdot \epsilon(\psi - \psi_i),$$

where the arguments τ and ψ are defined in (1); $l_i \in (0, 1)$ and $\psi_i \in [0, 2\pi)$ are some constants for each $i = \overline{1, m-1}$, with $\psi_i \neq \psi_j$ if $i \neq j$, and

$$\epsilon(\psi - \psi_i) \equiv \begin{cases} 0 & \text{if } \psi = \psi_i \\ 1 & \text{if } \psi \neq \psi_i, \end{cases}$$

then the corresponding plane figure P_m^* is:
1. a "simple star" with m "wings" or "vertices" when $\tau_* \equiv 0$ (see e.g. Figs. 1.e.);
2. a set of m segments of straight lines lying on the radii of a circle centered at the origin when $\tau_* > 0$ (see e.g. Fig. 1.f.).

REMARK 1. *In the case when $\psi_i \equiv 2\pi i/m$ and $l_i \equiv 1$, $\overline{i = 0, m-1}$, then P_m^* is a "regular simple star" (see Fig. 1.e.).*

- In this article PR_m^* is a "cylinder" with cross section a simple star, i.e.

$$(5) \qquad PR_m^* \equiv \bigcup_{i=0}^{m-1} T_i \equiv P_m^* \times [0, 2\pi) \equiv \bigcup_{i=0}^{m-1} \{I_i \times [0, 2\pi)\}$$

$$\equiv \left\{ (\tilde{x}_i = \tau l_i \cos \psi_i, \tilde{z}_i = \tau l_i \sin \psi_i, \theta) : \right.$$

$$\left. \tau \in [0, \tau^*]; \psi_i = \frac{2\pi i}{m}, i = \overline{0, m-1}; \theta \in [0, 2\pi] \right\}$$
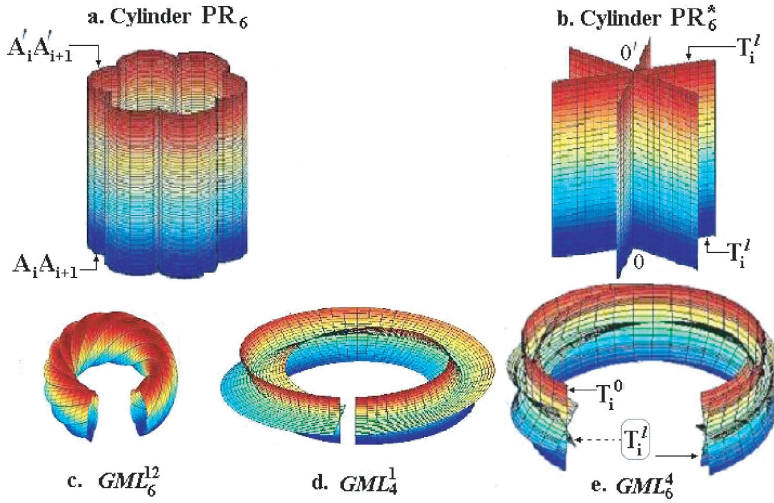
Figure 2

- T_i, for each $\overline{i = 0, m-1}$, is the wing of the cylinder PR_m^* corresponding to the angle ψ_i (see example in Fig. 2.b.), i.e.

$$T_i \equiv \{I_i \times [0, 2\pi)\} \equiv \{[0, l_i] \times [0, 2\pi)\}$$

(6)
$$I_i \equiv [0, l_i]$$

$$T_i^o \equiv \{I_i \times \{0\}\} \quad T_i^e \equiv \{I_i \times \{2\pi\}\}.$$

- I_i, $\overline{i = 0, m-1}$ is a wing of the plane figure P_m^*, and correspondingly $\tau \cdot l_i$ is its *"Length"* (see e.g. Fig. 1.e., 1.f. or Fig. 2.b., 2.d., 2.e.).
- $r(p,q)$ or $r(p)$—denotes the *"Radius"* of the plane figure P_m (for example, radius of the simple star in (2′)), defined by

(2^{**})
$$r(P_m^*) \equiv \max_{i = 0, m-1} \{\tau^* \cdot l_i\}$$

- OO'—is the axis of symmetry of the prism PR_m.

I. GENERALIZED MÖBIUS LISTING'S BODY

Generalized Twisting and Rotated bodies shortly GTR_m^n or bodies which are bounded by "Surfaces of revolution" are defined by different methods ([8], [15], [6] and some examples are shown in Fig. 2 and Fig. 3).

But in this article we consider a subset of the wide class GTR_m^n:—Generalized Möbius Listing's bodies, shortly GML_m^n.

DEFINITION 1. *A Generalized Möbius Listing's body—is obtained by identifying without deformation the opposite ends of the prism PR_m in such a way that:*
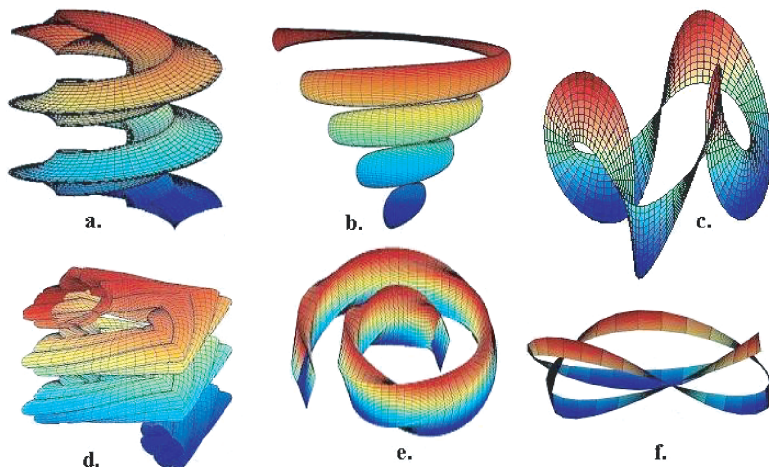
Figure 3

A) *For every integer $n \in \mathbb{Z}$ and $i = 0, \ldots, m - 1$ each vertex A_i coincides with $A'_{i+n} \equiv A'_{mod_m(i+n)}$, and each edge $A_i A_{i+1}$ coincides, correspondingly, with the edge*

$$A'_{i+n} A'_{i+n+1} \equiv A'_{mod_m(i+n)} A'_{mod_m(i+n+1)};$$

B) *The integer $n \in \mathbb{Z}$ denotes the number of rotations of the end of the prism with respect to the axis OO' before identification. If $n > 0$, the rotations are counter-clockwise, and if $n < 0$ then rotations are clockwise.*

Some particular examples of GML_3^n and their graphical realizations can be found in Fig. 2.c., 2.d., 2.e., Fig. 3.f., Fig. 4.a., or 4.b. More precise information about the structure of these bodies can be found in [7], [15], [18].

REMARK 2. *We can assert that:*
a.) *The GML_m^n body is a particular case of the GTR_m^n body.*
b.) *The basic line of a GML_m^n body, is always a closed line.*
c.) *The boundary of this body is a closed surface or line, and the parameters in its analytic representation depend on the indices of symmetry and the number or vertices of P_m (see [15]).*
d.) *The number n has a different meaning for each GML_m^n body, since it depends on the number m. When $n = m$ or $n = -m$ we have a full rotation of plane figures (in the radial cross section) around the basic line, correspondingly counter-clockwise or clockwise;*

DEFINITION 2. Rib *of the GML_m^n is a continuous closed line, in which are situated only the vertices of the radial cross sections (plane figures) of this body (see e.g. Fig. 4).*
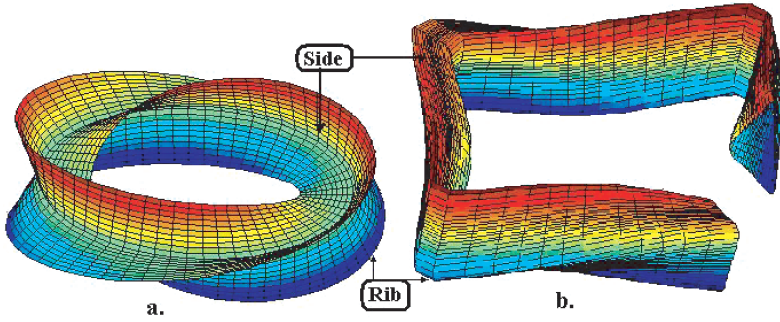
Figure 4

DEFINITION 3. Side *of the GML_m^n is a continuous closed surface, in which are situated only the edges of the radial cross section (plane figures) of this body (see e.g. Fig.* 4).

In this article, for simplicity but without loss of generality, we consider Generalized Möbius-Listing's bodies and surfaces GML_m^n with the following restrictions:

- The radial cross sections of these bodies usually are plane m-symmetric convex figures with m vertices (see e.g. Fig. 4.b.);
- The radial cross sections of these surfaces are plane m-symmetric star-like figures with m vertices (see e.g. Fig. 2 or Fig. 4.a.);
- The basic lines of these surfaces are always plane circles;
- The rule of twisting around the basic line is regular.

According to these restrictions the analytic representations of the corresponding GML_m^n bodies or surfaces have one of the following forms

$$X(\tau,\psi,\theta) = \left[R + p(\tau,\psi)\cos\left(\frac{n\theta}{m}\right) - q(\tau,\psi)\sin\left(\frac{n\theta}{m}\right)\right]\cos(\theta)$$

(7) $$Y(\tau,\psi,\theta) = \left[R + p(\tau,\psi)\cos\left(\frac{n\theta}{m}\right) - q(\tau,\psi)\sin\left(\frac{n\theta}{m}\right)\right]\sin(\theta)$$

$$Z(\tau,\psi,\theta) = p(\tau,\psi)\sin\left(\frac{n\theta}{m}\right) + q(\tau,\psi)\cos\left(\frac{n\theta}{m}\right),$$

where $p(\tau,\psi)$ and $q(\tau,\psi)$ are the functions in (2), or

$$X(\tau,\psi,\theta) = \left[R + p(\tau,\psi)\cos\left(\psi + \frac{n\theta}{m}\right)\right]\cos(\theta)$$

(8) $$Y(\tau,\psi,\theta) = \left[R + p(\tau,\psi)\cos\left(\psi + \frac{n\theta}{m}\right)\right]\sin(\theta)$$

$$Z(\tau,\psi,\theta) = p(\tau,\psi)\sin\left(\psi + \frac{n\theta}{m}\right),$$

where $p(\tau, \psi)$ is the function in (2^*) and τ, ψ, θ run in the parallelogram (1); the number m of vertices (and symmetry of the cross section) and the index of rotation n are arbitrary integer numbers. More precise information about the analytic representation of these bodies can be found in [15].

REMARK 3. *Note that:*

- 1. *For every n, the representation* (7), *is a one to one correspondence between the points of the cylinder PR_m and those of the GML_m^n body;*
- 2. *In particularly, if $n = 0$, equation (7) gives a one to one correspondence between the points of the cylinder PR_m and those of the GML_3^0 body, with identical radial cross sections;*
- 3. *The line $\{0\} \times [0, 2\pi) \subset PR_m$ is the origin (by correspondence (7)) of the basic line of the GML_m^n bodies.*
- 4. *Each point of the basic line is the center of symmetry of the radial cross section of the GML_m^n bodies.*

PROOF. We may remark that

$$(9) \qquad \frac{\partial(X, Y, Z)}{\partial(x, z, \theta)} = -R - \left[x \cos\left(\frac{n\theta}{m}\right) - z \sin\left(\frac{n\theta}{m}\right) \right] \neq 0,$$

where x and z are the functions in (2), i.e. the Jacobian determinant of this correspondence, according to the restriction $R > \tau^*$, is different from zero. Therefore, the relation (7) defines a one to one correspondence. Note that the last two parts of this Remark are trivial consequences of the relation (9).

The analytic representation (7) gives us possibility to discover some properties of the Generalized Möbius-Listing's bodies.

REMARK 4. *If the generalized Möbius-Listing's surface GML_m^n has a convex radial cross section (2) (or more generally the plane figure P_m satisfies star conditions and has smooth edges $A_i A_{i+1}$ for every $i = \overline{1, m-1}$), and if the integer number j— is the greatest common divisor of numbers m and $mod_m(n)$—then:*

- A.) *such GML_m^n body has a j-coloured surface (i.e. it is possible to paint the surface of this figure with j different colors without taking away the brush. It is prohibited to cross the edge of this figure);*
- A1.) *Each closed non-self-crossing line on the surface of the GML_m^n body, which is a parallel to the rib, is a $2\pi j$—periodic space line;*
- B.) *if $j = 1$, then the GML_m^n body has 1-coloured surface and its boundary edge is a closed line (see the classical Möbius strip);*
- C.) *if $n = m\omega$, $\omega = 0, 1, 2, \ldots$, then the GML_m^n body has an m-coloured surface; (see particular examples: 6-coloured surfaces in Fig. 2.c.);*
- D.) *In this article we consider Generalized Möbius-Listing's surface GML_m^n whose basic line is a 2π—periodic space line, like a circle;*
- E.) *if $n = \infty$ and its basic line is a smooth line, then the generalized Möbius-Listing's body is a "One-coloured" body—Torus without edges.*

PROOF. Without loss of generality we consider the analytic representation (7). According to these formulas, for each numbers m, n, the following identities hold

$$X(\tau, \psi, 2\pi) = X\left(\tau, \psi + \frac{2\pi n}{m}, 0\right)$$

(10)
$$Y(\tau, \psi, 2\pi) = Y\left(\tau, \psi + \frac{2\pi n}{m}, 0\right)$$

$$Z(\tau, \psi, 2\pi) = Z\left(\tau, \psi + \frac{2\pi n}{m}, 0\right),$$

or, in particular, for each numbers m, n and i

(11)
$$X(\tau, \psi_i, 2\pi) = X(\tau, \psi_{mod_m(i+n)}, 0)$$
$$Y(\tau, \psi_i, 2\pi) = Y(\tau, \psi_{mod_m(i+n)}, 0)$$
$$Z(\tau, \psi_i, 2\pi) = Z(\tau, \psi_{mod_m(i+n)}, 0).$$

The geometric meaning of this relation is that, after bending the cylinder PR_m, each edge $A_i A_{i+1}$ coincides with the edge $A'_{mod_m(i+n)} A'_{mod_m(i+n+1)}$. But this is the condition A) in the definition 1. Consequently, it is possible to write the following permutation

(12)
$$A_0 A_1 \rightarrow A'_{mod_m(n)} A'_{mod_m(n+1)}$$
$$A_1 A_2 \rightarrow A'_{mod_m(n+1)} A'_{mod_m(n+2)}$$
$$\dots\dots\dots\dots\dots\dots\dots\dots\dots\dots$$
$$A_{m-2} A_{m-1} \rightarrow A'_{mod_m(n+m-2)} A'_{mod_m(n+m-1)}.$$

But, according to a well known theorem, such permutations can be constructed with exactly $gcd(m, mod_m(n))$ numbers of disjoint cycles (gcd denotes the greatest common divisor). The number of these cycles is the number of different colors we can put on the surface of this GML_m^n body. The other different items of this remark are simple corollaries of the relation (12).

II. RELATIONS BETWEEN THE SET OF GENERALIZED MÖBIUS-LISTING'S SURFACES AND THE SETS OF RIBBON KNOTS AND RIBBON LINKS

The results described in this chapter were already considered in previous articles for GML_m^n surfaces for arbitrary m (see [18], [19]). In this article, in order to simplify the proofs of our main results and to compare the Generalized Möbius-Listing's surfaces results with those of bodies, we recall (without proof) the definitions and theorems, particularly for the Generalized Möbius-Listing's surfaces GML_3^n and for the ribbon links which appear after their cutting processes.

We use the following definitions and notations:

DEFINITION 4. *A closed line (similar to the rib or basic line), which is situated on a GML_3^n and is ''parallel'' to the basic (or rib's) line of the GML_3^n (i.e. the distance*
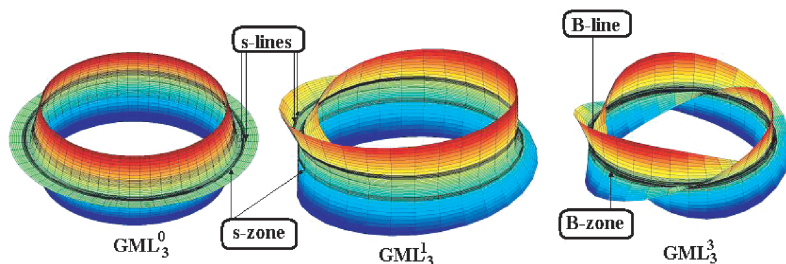
Figure 5

between this line and basic or rib's lines is constant) is called a "Slit line" or shortly an "s-line".

- *If the distance between an s-line and the basic line is zero, then this s-line coincides with the basic line (and is called "B-line").*

DEFINITION 5. *A domain situated on the surface (or side) GML_3^n and such that its border's lines are slit lines, is called a "Slit zone" or shortly an "s-zone".*

- *The distance between the border's lines of an s-zone is the "width" of this s-zone.*
- *If an s-zone's width equals to zero, then this zone reduces to an s-line.*

DEFINITION 6. *If the "B-line" is properly contained inside a "Slit zone"—i.e. the distance to the border's lines is strictly positive—then this "Slit zone" is called a "B-zone".*

- *A B-zone has a "Radius"—which is the maximal distance between the basic line and the border line of this zone (see e.g. Fig. 5.c.).*

DEFINITION 7. *The "process of cutting" or shortly the "cutting" is always realized along some s-lines and produces the vanishing (i.e. elimination) of the corresponding s-zone (which possibly reduces to an s-line).*

- *If a GML_3^n surface is cut along an s-line, non coinciding with the B-line (process denoted by the symbol: $\rightarrow^1$), then the resulting object is called an "s-slitting GML_3^n" and the corresponding vanishing zone is called an* s-slit.
- *If a GML_3^n surface is cut along its B-line (process denoted by the symbol: $\rightarrow^B$), then the resulting object is called a "B-slitting GML_3^n" and the corresponding vanishing zone is called a* B-slit.
- *If the vanishing zone—after an* s-slit *(a* B-slit*)—is given by an "s-zone" (a "B-zone"), then the cutting process is called an* s-zone-slit *(a* B-zone-slit*).*

REMARK 5. *Note that:*

- A. *In this article, we use the terms "Ribbon link-1" or "Bulk link-1" for denoting correspondingly "Ribbon knot" or "Bulk knot";*

- B. *The indices of corresponding bulk or ribbon links coincide with those of the classical links tabulation* (*thread structure without interior geometry see e.g.* [4], [9], [20],...) *with an important exception;*
- C. *We distinguish ribbon* (*or bulk*) *link-1* $\{0_1\}$ (*basic line of this object is a plane closed line similar to a circle*) *and ribbon link-1* $\{1_1\}$ (*basic line of this object is a space closed line similar to the rib of a classical Möbius strip*)*!*

THEOREM 1. *If the GML_3^n surface is cut along a non trivial s-line* (*i.e. a line which does not coincide with its basic line*), *then for each integer number n, after an s-zones-slit, an object ''ribbon link-2'' appears, whose one component is a ribbon link-1* $\{0_1\}$ (*indices are defined according to the known tabulation for knots and links of small complexity see e.g.* [4], [9], [20],...) *of the GML_3^n surface, and the other components are:*

A. *ribbon link-1* $\{0_1\}$ *of the $GML_2^{2\omega}$ surfaces—if $n = 3\omega$* ($\omega \in \mathbf{Z}$), *i.e. in this case*

$$(13) \qquad GML_3^{3\omega} \to^1 \text{ribbon link-2 } (2\omega)_1^2 \text{ of the } GML_3^{3\omega} \text{ and } GML_2^{2\omega}.$$

A particular case, when $\omega = 2$, is shown in Fig. 6.a.;

B. *ribbon link-1* $\{(4\omega + 1)_1\}$ (*see Remark 5. C.*) *of the $GML_2^{2\cdot3(\omega+1)}$ surfaces—if $n = 3\omega + 1$, i.e. in this case*

$$(14) \qquad GML_3^{3\omega+1} \to^1 \text{ribbon link-2 of the } GML_3^{3\omega+1} \text{ and } GML_2^{6\omega+6}.$$

A particular case, when $\omega = 0$, is shown in Fig. 7.a.;

C. *ribbon link-1* $\{(4\omega + 3)_1\}$ *of the $GML_2^{2\cdot3(\omega+1)+2}$ surfaces—if $n = 3\omega + 2$, i.e. in this case*

$$(15) \qquad GML_3^{3\omega+2} \to^1 \text{ribbon link-2 of the } GML_3^{3\omega+2} \text{ and } GML_2^{6\omega+8}.$$

A particular case, when $\omega = 1$, is shown in Fig. 8.a.;

THEOREM 2. *If the GML_3^n surface is cut along a B-line, then for each integer number n, after a B-zone-slit:*

A. *if $n = 3\omega$, an object ''ribbon link-3'' appears, each component of this object is a ribbon link-1* $\{0_1\}$ *of the $GML_2^{2\omega}$ surface; i.e. for each $\omega = 0, 1, 2, \ldots,$*

$$(16) \qquad\qquad GML_3^{3\omega} \to^b \text{ribbon link-3 of the } 3 \times GML_2^{2\omega}.$$

A particular case, when $\omega = 2$, is shown in Fig. 6.b.;

B. *if $n = 3\omega + 1$, then an object ''ribbon link-1''* $\{(4\omega + 1)_1\}$ (*see Remark 5. C.*) *of the $GML_2^{2\cdot3(\omega+1)}$ surface appears; i.e. for each natural $\omega = 0, 1, 2, \ldots,$*

$$(17) \qquad GML_3^{3\omega+1} \to^b \text{ribbon link-1 } \{(4\omega + 1)_1\} \text{ of the } GML_2^{6\omega+6}.$$

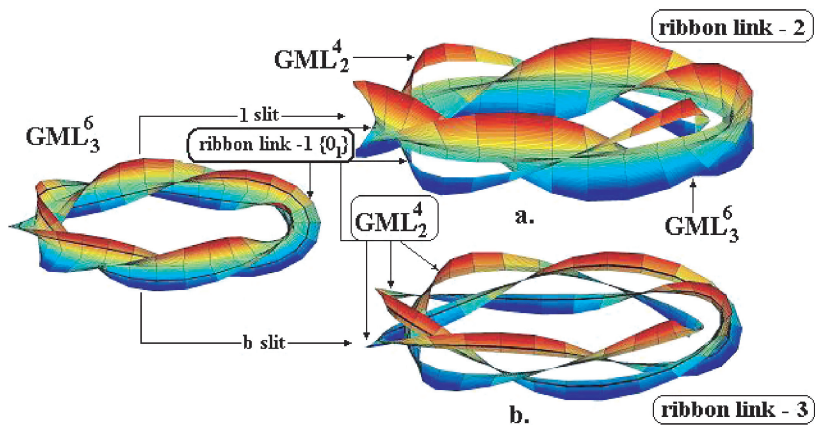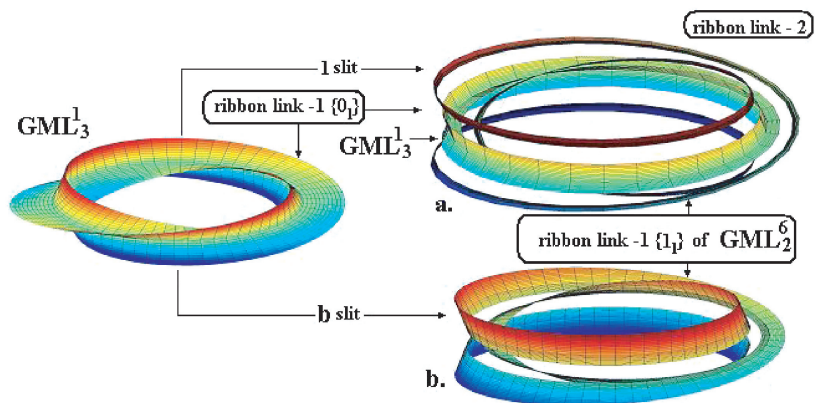*A particular case, when $\omega = 0$, is shown in Fig. 7.b.;*

Figure 6

Figure 7

C. *if $n = 3\omega + 2$, then an object* "ribbon link-1" $\{(4\omega + 3)_1\}$ *of the $GML_2^{2 \cdot 3(\omega+1)+2}$ surface appears; i.e. for each natural $\omega = 0, 1, 2, \ldots$,*

$$(18) \qquad GML_3^{3\omega+2} \rightarrow^b ribbon\ link\text{-}1\ \{(4\omega + 3)_1\}\ of\ the\ GML_2^{6\omega+8}.$$

A particular case, when $\omega = 1$, is shown in Fig. 8.b.

In general the corresponding indices of the link-2 group, appearing after an *s*-zone or *b*-zone slits of a GML_2^n surface, is at present unknown (only in some particular cases, when we have the possibility to perform a direct observation, we know the indices of resulting objects (e.g. Theorem 1, when $\omega = 0$: in case A., a link-2 $\{0_1^2\}$).
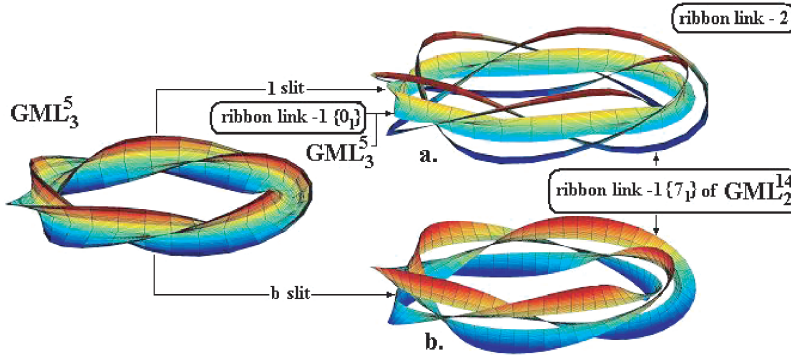
Figure 8

III. Relations between the set of Generalized Möbius-Listing's Bodies and the sets of Bulky Knots and Bulky Links

In this section, we consider Generalized Möbius-Listing's Bodies whose radial cross sections are convex 3-angular and 3-symmetric plane figures.

DEFINITION 8. *We call* Slit-surface *of the* GML_3^n *body a surface* GML_2^k *such that:*

1. *The basic line is strictly contained into the* GML_3^n *body and it is ''parallel'' to the basic line and ribs of this body;*
2. *The radial cross section is a straight line;*
3. *The line of intersection of the* GML_2^k *with the* GML_3^n *body, situated on the side of this body, is ''parallel'' to the rib line of the* GML_3^n *body. This restriction defines the number k of rotations (of surface) which strictly depends on the number of rotation n, of the body;*

DEFINITION 9. *We will use the following notations:*

- a. SVB-surface *of the* GML_3^n *body is a slit-surface, whose radial cross section (straight line) contains a vertex and the center of symmetry of the radial cross section of the* GML_3^n *body (see e.g. Fig. 9.a.);*
- b. SB-surface *of the* GML_3^n *body is a slit-surface, whose radial cross section (straight line) contains the center of symmetry and does not contain vertices of the radial cross section of the* GML_3^n *body (see e.g. Fig. 9.b.);*
- c. SV-surface *of the* GML_3^n *body is a slit-surface, whose radial cross section (straight line) contains a vertex and does not contain the center of symmetry of the radial cross section of the* GML_3^n *body (see e.g. Fig. 9.c.);*
- d. SV$_{ij}$-surface *of the* GML_3^n *body is a slit-surface, whose radial cross section (straight line) contains two vertices of the radial cross section of the* GML_3^n *body (see e.g. Fig. 9.d.). If the cross section is a triangle then this surface coincides with the corresponding side of* GML_3^n *body;*
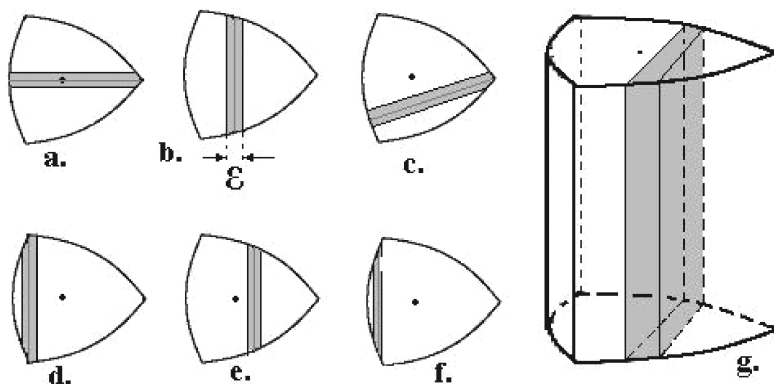
Figure 9

- e. S_{ij}-surface *of the* GML_2^n *body is a slit-surface such that the ends of the straight line* (*radial cross section*) *are situated on the edges, correspondingly with labels i and j, of plane figures of the radial cross section of* GML_3^n *body* (*see e.g.* S_{ii}-*surface in Fig.* 9.f. *and* S_{ij}-*surface* ($i \neq j$) *in Fig.* 9.e.). *If the cross section is a triangle then this surface coincides with the corresponding side of* GML_3^n *body;*

DEFINITION 10. *A domain, part of the* GML_3^n *body* (*having structure similar to a* GML_4^k *body*), *whose two opposite parallels to the side-surfaces* (*see Def.* 3) *are slit-surfaces, is called a* "Slit zone" *or shortly an* "s-zone".

- *"Thickness" of the slit-zone is the distance between two opposite parallel slit-surfaces* (*distance between two opposite parallel straight line in the radial cross section of the slit-zone, see e.g. Fig.* 9.b.)*;*
- *If the thickness of a slit-zone is zero, then it coincides with a slit-surface.*

    Without loss of generality, in this article we assume that the ε-thickness of the slit-zone is very small with respect to the size of the body, i.e. $0 \leq \varepsilon \ll r(p)$.

DEFINITION 11. *The* "process of cutting" *or shortly the* "cutting" *of a* GML_3^n *body is always realized along some s-surface and produces the vanishing* (*i.e. elimination*) *of the corresponding s-zone* (*which possibly reduces to a slit-surface*).

- *If a* GML_3^n *body is cut along an SVB-surface* ($\rightarrow^{SVB}$), *then the corresponding vanishing zone is called an* SVB-slit, *and such cutting process is called an* SVB-zone-slit;
- *If a* GML_3^n *body is cut along its SB-surface* ($\rightarrow^{SB}$), *then the corresponding vanishing zone is called a* SB-slit, *and such cutting process is called an* SB-zone-slit;
- *If a* GML_3^n *body is cut along its SV-surface* ($\rightarrow^{SV}$), *then the corresponding vanishing zone is called a* SV-slit, *and such cutting process is called an* SV-zone-slit;

- If a GML_3^n body is cut along its SV_{ij}-surface ($\rightarrow^{SV_{ij}}$), then the corresponding vanishing zone is called a SV_{ij}-slit, and such cutting process is called an SV_{ij}-zone-slit;
- If a GML_3^n body is cut along its S_{ij}-surface ($\rightarrow^{S_{ij}}$), then the corresponding vanishing zone is called an S_{ij}-slit ($i, j = 0, 1$), and such cutting process is called an S_{ij}-zone-slit.

REMARK 6. *If the radial cross section of the GML_3^n body is a triangle, then S_{ii}-zone-slit or SV_{ij}-zone-slit are impossible.*

After an S_{ij}-zone-slit ($i \neq j$) of the GML_3^n body, four different cases appear, which depend on the position of the cross section of the slit-surface over the cross section of the body (*position of straight line inside the triangular planar figure*):

1. S_{ij}^*-zone-slit—*straight line is between the vertex and nearby the ''middle line''* (*line which connects two middle point of the opposite sides*) *of planar figure of the radial cross section of the body;*
2. $S_{ij}^{\#}$-zone-slit—*straight line coincides with the ''middle line'' of planar figure of the radial cross section of the body;*
3. $S_{ij}^{\flat}$-zone-slit—*straight line is between the center of symmetry and ''middle line'' of planar figure of the radial cross section of the body;*
4. S_{ij}'-zone-slit—*straight line is between the center of symmetry and the side of planar figure of the radial cross section of the body;*

By recalling the Remark 3 and using the previous theorems, we can prove the following results for the Generalized Möbius-Listing's Bodies GML_3^n with *convex* 3-symmetric and 3-*angular* radial cross sections.

THEOREM 3. *If the number of twisting is $n \equiv 3\omega$, where $\omega \in \mathbf{Z}$ denotes the number of full rotations, and the GML_3^n body is cut along some of its slit-surfaces, then an object ''bulk link-2'' $\{(2\omega)_1^2\}$ of the bulk link-1, with structure $\{0_1\}$, appears* (*see Remark 5.*)*; but the components of this bulk link-2 have different structure, more precisely:*

***Case A.** after an* SVB-zone-slit *or* SV-zone-slit *of the GML_3^n body, an object bulk link-2 $\{(2\omega)_1^2\}$ of the GML_3^n bodies appears, whose radial cross sections are three angular plane figures, i.e. for each natural $\omega = 0, 1, 2, \ldots$*

$$(19) \qquad GML_3^{3\omega} \rightarrow^{SVB \text{ or } SV} link\text{-}2\{(2\omega)_1^2\} \text{ of the two } GML_3^{3\omega};$$

***Case B.** after an* SB-zone-slit *or an* S_{ij}-zone-slit *($i \neq j$ and $i, j = 0, 1, 2$) of the GML_3^n body, an object bulk link-2 $\{(2\omega)_1^2\}$ of the $GML_3^{3\omega}$ and $GML_4^{4\omega}$ bodies appears, whose radial cross sections are correspondingly three and four angular plane figures, i.e. for each natural $\omega = 0, 1, 2, \ldots$*

$$(20) \qquad GML_3^{3\omega} \rightarrow^{SB \text{ or } S_{ij}} link\text{-}2 \{(2\omega)_1^2\} \text{ of the } GML_3^{3\omega} \text{ and } GML_4^{4\omega};$$

Case C. *after an SV_{ij}-zone-slit of the GML_3^n body, an object bulk link-2 $\{(2\omega)_1^2\}$ of the $GML_3^{3\omega}$ and $GML_2^{2\omega}$ bodies appears, whose radial cross sections are correspondingly three and two angular plane figures, i.e. for each natural $\omega = 0, 1, 2, \dots$*

$$(21) \qquad GML_3^{3\omega} \to^{SV_{ij}} \text{ link-2 } \{(2\omega)_1^2\} \text{ of the } GML_3^{3\omega} \text{ and } GML_2^{2\omega};$$

Case D. *after an S_{ii}-zone-slit of the GML_3^n body, an object bulk link-2 $\{(2\omega)_1^2\}$ of the GML_2^n and $GML_5^{5\omega}$ bodies appears, whose radial cross sections are correspondingly two and five angular plane figures, i.e. for each natural $\omega = 0, 1, 2, \dots$*

$$(22) \qquad GML_3^{3\omega} \to^{S_{ii}} \text{ link-2} \{(2\omega)_1^2\} \text{ of the } GML_2^{2\omega} \text{ and } GML_5^{5\omega}.$$

PROOF. According to the transformation (7) or (8), the origin of the Generalized Möbius-Listing's body GML_2^n is a cylinder, whose cross section is similar to the radial cross section of the considered body. So that, we can consider this cylinder as the union of parallel rectangles, whose two opposite sides are element of the cylinder (generatrix) and the remaining two ones are situated on the opposite ends of the cylinder (geometrically identical to its cross section) (see e.g. Fig. 9.g.). In this case each rectangle defines (by (7)) a Generalized Möbius-Listing's surface GML_2^n. Also ω is the number of full rotations of this body, so that each element of the geometric object which appears after cutting makes ω rotations around its basic line and this means that each element makes ω coils around second elements, so that a link-2 $\{(2\omega)_1^2\}$ appears. Difference between the considered cases are the shapes of radial cross sections of the geometric objects appearing after cutting. This is the basis for proving our theorem.

Case A. We may consider the cylinder as the union of parallel rectangles, orthogonal to the rectangle origin of the SVB-surface (see e.g. Fig. 9.g.). The SVB-surface includes one rib of the GML_3^n body and the opposite side of this surface cuts the side of the GML_3^n body, so after an SVB-zone-slit, new ribs appear (generated by new angular points on the radial cross section). So that, in this particular case, each rectangle defining the Generalized Möbius-Listing's surface GML_2^n is cut along its basic line. According to the Theorem 1 case A. (see [12]), and representation (7) or (8), it is easy to show that after an SVB-*zone-slit* of the GML_3^n body, an object bulk link-2 $\{(2\omega)_1^2\}$ of GML_3^n bodies appears, whose radial cross sections are three angular plane figures. This result is formally similar to the results of the Theorem 1 case A., for GML_2^n surfaces (see [7]).

Examples of shapes of the radial cross sections before and after SVB-zone-slits are shown in the table of Fig. 10., row a., but a particular example of the objects before and after cutting, when $\omega = 2$ are shown in Fig. 11 (general views of these objects are similar for each cases and only differences are the shapes of cross sections in the resulting bulk link-2. See e.g. Fig. 11.b.).

Cases B.–D. The process of proving other cases is essentially similar to the preceding one. But now, we must consider the different variants appearing after cutting a plane triangular convex figure by a straight line and after considering the corresponding cylinder (origin of the Generalized Möbius-Listing's body GML_3^n) as the union of parallel rectangles. So that, we can always correspond-

Shapes of radial cross section $GML_3^{3\omega}$		– slit	Parameters of the objects which appear after cutting			
			Shapes of radial cross sections	Structure of elements	Link group of elements	Link group of object
a.		SVB		$GML_3^{3\omega}$ $GML_3^{3\omega}$		
b.		SB		$GML_4^{4\omega}$ $GML_3^{3\omega}$		
c1		SV_i		$GML_4^{4\omega}$ $GML_2^{2\omega}$		
c.		SV		$GML_3^{3\omega}$ $GML_3^{3\omega}$	link-1 $\{0_1\}$	link-2 $\{(2\omega)_1^2\}$
d.		SV_{ij}		$GML_2^{2\omega}$ $GML_3^{3\omega}$		
e.		S_{ij}		$GML_4^{4\omega}$ $GML_3^{3\omega}$		
f.		S_{ii}		$GML_2^{2\omega}$ $GML_5^{5\omega}$		

Figure 10

ingly apply the results of cases A., of the Theorem 1 or Theorem 2 (see [7]). According to these results, the bulk link-2 have identical indices $(2\omega)_1^2$, but different shapes of their radial cross sections, which depend on the position of the slit-surfaces (position of the corresponding straight line with respect to the radial cross sections of the GML_3^n bodies—see e.g. Figs. 9.a.–9.f.). So, we have proved all cases of Theorem 3. All possible cases and corresponding shapes of the radial cross sections before and after the cutting process are given in the table of Fig. 10.

THEOREM 4. *If the number of twisting is $n \equiv 3\omega + 1$, where ω is an arbitrary integer number, and the GML_3^n body is cut along some of its slit-surfaces, then nine different cases appear:*

***Case A.** after an* SVB-zone-slit *of the GML_3^n body, an object bulk link-2, of the $GML_3^{3\cdot3(\omega+1)}$ bodies appears, whose components are bulk link-1 $\{(4\omega+1)_1\}$ (see*
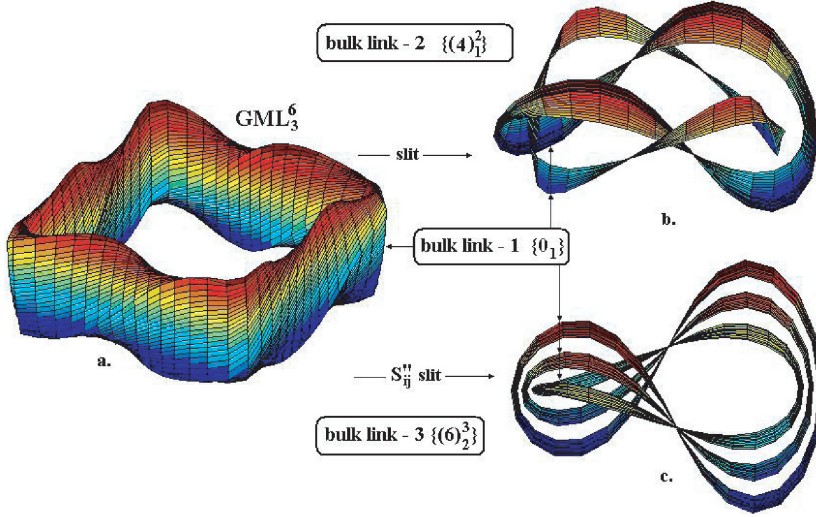
Figure 11

Remark 5. C.), *and their radial cross sections are three angular mirror symmetric plane figures, i.e. for each natural $\omega = 0, 1, 2, \ldots$*

$$(23) \qquad GML_3^{3\omega+1} \to^{SVB} \text{ link-2 of the 2 } GML_3^{9\omega+9};$$

Case B. *after an* SB-zone-slit *of the GML_3^n body, an object bulk link-2, of the $GML_3^{3\cdot3(\omega+1)}$ and $GML_4^{3\cdot4(\omega+1)}$ bodies appears, whose components are bulk link-1 $\{(4\omega+1)_1\}$ (see Remark 5. C.), and their radial cross sections correspondingly are three and four angular plane figures, i.e. for each natural $\omega = 0, 1, 2, \ldots$*

$$(24) \qquad GML_3^{3\omega+1} \to^{SB} \text{ link-2 of the } GML_3^{9\omega+9} \text{ and } GML_4^{12\omega+12};$$

Case C. *after an* SV-zone-slit *of the GML_3^n body, an object bulk link-3 appears. One component of this object is a bulk link-1 $\{0_1\}$ of the $GML_3^{3\omega+1}$ body, the second and third are bulk link-1 $(4\omega+1)_1$ (see Remark 5. C.) of the $GML_3^{3?3(\omega+1)}$ and $GML_4^{3?4(\omega+1)}$ bodies, whose radial cross sections correspondingly are three and four angular plane figures; i.e. for each natural $\omega = 1, 2, \ldots$*

$$(25) \qquad \begin{array}{c} GML_3^{3\omega+1} \to^{SV} \text{ link-3 of the } GML_3^{3\omega+1}, \\ GML_3^{9\omega+9} \text{ and } GML_4^{12\omega+12}; \end{array}$$

Case D. *after an SV_{ij}-zone-slit of the GML_3^n body, an object bulk link-2 appears. One component of this object is a bulk link-1 $\{0_1\}$ of the $GML_3^{3\omega+1}$ body and the second is a bulk link-1 $\{(4\omega+1)_1\}$ (see Remark 5. C.) of the $GML_2^{3\cdot2(\omega+1)}$ bodies,*

whose radial cross sections correspondingly are three and two angular plane figures; i.e. for each natural $\omega = 1, 2, \ldots$

$$(26) \qquad GML_3^{3\omega+1} \to^{SV_{ij}} \textit{link-2 of the } GML_3^{3\omega+1} \textit{ and } GML_2^{6\omega+6};$$

Case E1. *after an S_{ij}^*-zone-slit of the GML_3^n body, an object bulk link-2 appears. One component of this object is a bulk link-1 $\{0_1\}$ of the $GML_6^{6\omega+2}$ body and the second is a bulk link-1 $\{(4\omega+1)_1\}$ (see Remark 5. C.) of the $GML_3^{3\cdot3(\omega+1)}$ bodies, whose radial cross sections correspondingly are six and three angular plane figures; i.e. for each natural* $\omega = 1, 2, \ldots$

$$(27) \qquad GML_3^{3\omega+1} \to^{S_{ij}^*} \textit{link-2 of the } GML_6^{6\omega+2} \textit{ and } GML_3^{9\omega+9};$$

Case E2. *after an $S_{ij}^{\#}$-zone-slit of the GML_3^n body, an object bulk link-2 appears. One component of this object is a bulk link-1 $\{0_1\}$ of the $GML_3^{3\omega+1}$ body and the second is a bulk link-1 $\{(4\omega+1)_1\}$ (see Remark 5. C.) of the $GML_3^{3\cdot3(\omega+1)}$ bodies, whose radial cross sections correspondingly are six and three angular plane figures; i.e. for each natural* $\omega = 1, 2, \ldots$

$$(28) \qquad GML_3^{3\omega+1} \to^{S_{ij}^{\#}} \textit{link-2 of the } GML_3^{3\omega+1} \textit{ and } GML_3^{9\omega+9};$$

Case E3. *after an $S_{ij}^{\flat}$-zone-slit of the GML_3^n body, an object bulk link-3 appears. One component of this object is a bulk link-1 $\{0_1\}$ of the $GML_3^{3\omega+1}$ body and the second and third ones are bulk link-1 $\{(4\omega+1)_1\}$ (see Remark 5. C.) of the $GML_3^{3\cdot3(\omega+1)}$ and $GML_5^{3\cdot5(\omega+1)}$ bodies, whose radial cross sections correspondingly are three and five angular plane figures; i.e. for each natural* $\omega = 1, 2, \ldots$

$$(29) \qquad \begin{array}{c} GML_3^{3\omega+1} \to^{S_{ij}^{\flat}} \textit{link-3 of the } GML_3^{3\omega+1}, \\ GML_3^{9\omega+9} \textit{ and } GML_5^{15\omega+15}; \end{array}$$

Case E4. *after an $S_{ij}^{!}$-zone-slit of the GML_3^n body, an object bulk link-3 appears. One component of this object is a bulk link-1 $\{0_1\}$ of the $GML_3^{3\omega+1}$ body and the second and third ones are bulk links-1 $\{(4\omega+1)_1\}$ (see Remark 5. C.) of the $GML_4^{3\cdot4(\omega+1)}$ bodies, whose radial cross sections are four angular plane figures; i.e. for each natural* $\omega = 1, 2, \ldots$

$$(30) \qquad \begin{array}{c} GML_3^{3\omega+1} \to^{S_{ij}^{!}} \textit{link-3 of the } GML_3^{3\omega+1}, \\ GML_4^{12\omega+12} \textit{ and } GML_4^{12\omega+12}; \end{array}$$

Case F. *after an S_{ii}-zone-slit (for any $i = 0, 1, 2$) of the GML_3^n body, an object bulk link-2 appears. One component of this object is a bulk link-1 $\{0_1\}$ of the $GML_9^{3(3\omega+1)}$ body and the second is a bulk link-1 $\{(4\omega+1)_1\}$ (see Remark 5. C.) of the $GML_2^{3\cdot2(\omega+1)}$ body; i.e. for each natural* $\omega = 1, 2, \ldots$

$$(31) \qquad GML_3^{3\omega+1} \to^{S_{ii}} \textit{link-2 of the } GML_9^{9\omega+3} \textit{ and } GML_6^{6\omega+6}.$$

PROOF. According to the transformation (7) or (8), the origin of the Generalized Möbius-Listing's body GML_3^n is a cylinder whose cross section is similar to the radial cross section of the considered body. But now, after transformation, taking into account the 3-symmetry of the cross section, after a $120°$ degree turning, the ends of this cylinder identify. So that, we can consider this cylinder as the union of parallel rectangles, whose opposite sides are elements of the cylinder (generatrix) and the remaining two ones are situated on the opposite ends of the cylinder (geometrically identical to its cross section). In this case each rectangle is defined by (7), and the process of cutting "is completed" after $3 \cdot 360°$ degree turning (Remark 2. see [15]). According to this result two types of Generalized Möbius-Listing's bodies with strongly different structure of their basic line appear:

1. the basic line is a circle (similar to the basic line of the initial body); This object contains the "old basic line";
2. the basic line makes $3\omega + 1$ coils around the "small part" of some classical torus, after making three circuits around the "big parts". This is the basis for proving the above theorem.

Case A. We may consider cylinder as the union of parallel rectangles, orthogonal to the rectangle, origin of the SVB-surface. The SVB-surface includes one of the ribs of GML_3^n bodies, and after an SVB-zone-slit, only one new rib appears (generated by new angular points on the radial cross section). So that, in this particular case, each rectangle defining the Generalized Möbius-Listing's surface GML_3^n is cut along its basic line. According to the representation (7) or (8), it is easy to show that, after an SVB-zone-slit of the GML_3^n body, two objects, bulk link-1 $\{(4\omega + 1)_1\}$ (see Remark 5.C.) of the GML_3^n bodies appear, whose radial cross sections are three angular plane mirror symmetric figures. Examples of the shapes of the radial cross sections before and after SVB-zone-slit are shown in Fig. 12.

Case B. Analogously to the preceding case, after similar considerations, we could find results for SB-zone-slits, but in this case, according to the 3-symmetry of the radial cross section, we must only remark that the rectangle (origin of the SB-zone-slit) divides the cylinder in two different parts and, after transformation (7), these two parts yield two bulk link-1, whose radial cross sections consist in three and four angular plane figures. Examples of shapes of the radial cross sections, before and after an SB-zone-slit, are shown in corresponding rows of the table in Fig. 12.

Case C., D., E., or F. In these seven cases, the arguments for proving our results are essentially similar to those used in Theorem 2, case B.

Unfortunately we do not know, at present, what is the precise type of the final links (according to the classic knots tabulation—see e.g. [4], [9], [20], ... and Fig. 13.) (which is the same for these nine cases), appearing after the corresponding zone-slit of a GML_3^n.

In these nine cases only *three different* types of links appear (particular examples of the results of Theorem 4., when $\omega = 0$, are shown in:

Shapes of radial cross section GML_3^n	- slit	Parameters of the objects which appear after cutting			
		Shapes of radial cross sections	if $n=3\omega+1$ object is / Link group of elements	if $n=3\omega+2$ object is / Link group of elements
A.	SVB		link-2 of $GML_3^{9\omega+9}$ / $GML_3^{9\omega+9}$ link-1 $\{(4\omega+1)_1\}$ / $\{(4\omega+1)_1\}$	link-2 of $GML_3^{9\omega+12}$ / $GML_3^{9\omega+12}$ link-1 $\{(4\omega+3)_1\}$ / $\{(4\omega+3)_1\}$
B.	SB		link-2 of $GML_3^{9\omega+9}$ / $GML_4^{12\omega+12}$ $\{(4\omega+1)_1\}$ / $\{(4\omega+1)_1\}$	link-2 of $GML_3^{9\omega+12}$ / $GML_4^{12\omega+16}$ $\{(4\omega+3)_1\}$ / $\{(4\omega+3)_1\}$
C.	SV		link-3 of $GML_3^{3\omega+1}$ / $GML_3^{9\omega+9}$ / $GML_4^{12\omega+12}$ $\{0_1\}$ / $\{(4\omega+1)_1\}$ / $\{(4\omega+1)_1\}$	link-3 of $GML_3^{3\omega+2}$ / $GML_3^{9\omega+12}$ / $GML_4^{12\omega+16}$ $\{0_1\}$ / $\{(4\omega+3)_1\}$ / $\{(4\omega+3)_1\}$
D.	$SV_{\ddot{ij}}$		link-2 of $GML_3^{3\omega+1}$ / $GML_2^{6\omega+6}$ $\{0_1\}$ / $\{(4\omega+1)_1\}$	link-2 of $GML_3^{3\omega+2}$ / $GML_2^{6\omega+8}$ $\{0_1\}$ / $\{(4\omega+3)_1\}$
D1	$SV_{\dot{i}}$		link-2 of $GML_6^{6\omega+2}$ / $GML_2^{6\omega+6}$ $\{0_1\}$ / $\{(4\omega+1)_1\}$	link-2 of $GML_6^{6\omega+4}$ / $GML_2^{6\omega+8}$ $\{0_1\}$ / $\{(4\omega+3)_1\}$
E1	$S^{*}_{\ddot{ij}}$		link-2 of $GML_6^{6\omega+2}$ / $GML_3^{9\omega+9}$ $\{0_1\}$ / $\{(4\omega+1)_1\}$	link-2 of $GML_6^{6\omega+4}$ / $GML_3^{9\omega+12}$ $\{0_1\}$ / $\{(4\omega+3)_1\}$
E2	$S^{\#}_{\ddot{ij}}$		link-2 of $GML_3^{3\omega+1}$ / $GML_3^{9\omega+9}$ $\{0_1\}$ / $\{(4\omega+1)_1\}$	link-2 of $GML_3^{3\omega+2}$ / $GML_3^{9\omega+12}$ $\{0_1\}$ / $\{(4\omega+3)_1\}$
E3	$S^{\flat}_{\ddot{ij}}$		link-3 of $GML_3^{3\omega+1}$ / $GML_3^{9\omega+9}$ / $GML_5^{15\omega+15}$ $\{0_1\}$ / $\{(4\omega+1)_1\}$ / $\{(4\omega+1)_1\}$	link-3 of $GML_3^{3\omega+2}$ / $GML_3^{9\omega+12}$ / $GML_5^{15\omega+20}$ $\{0_1\}$ / $\{(4\omega+3)_1\}$ / $\{(4\omega+3)_1\}$
E4	$S^{\prime}_{\ddot{ij}}$		link-3 of $GML_3^{3\omega+1}$ / $GML_4^{12\omega+12}$ / $GML_4^{12\omega+12}$ $\{0_1\}$ / $\{(4\omega+1)_1\}$ / $\{(4\omega+1)_1\}$	link-3 of $GML_3^{3\omega+2}$ / $GML_4^{12\omega+16}$ / $GML_4^{12\omega+16}$ $\{0_1\}$ / $\{(4\omega+3)_1\}$ / $\{(4\omega+3)_1\}$
F.	$S_{\ddot{ii}}$		link-2 of $GML_2^{6\omega+6}$ / $GML_9^{9\omega+3}$ $\{(4\omega+1)_1\}$ / $\{0_1\}$	link-2 of $GML_2^{6\omega+8}$ / $GML_9^{9\omega+6}$ $\{(4\omega+3)_1\}$ / $\{0_1\}$

Figure 12

– Fig. 13. b., which corresponds to the cases A. and B.;
– Fig. 13. c., which corresponds to the cases D., E1., E2., F.;
– Fig. 13. d., which corresponds to the cases C., E3., E4.).

Also different are the polygons generated in the radial cross sections of the bulk links components, which depend on the position of the origin with respect to the corresponding slit-surfaces in the cylinder (or on the position of the
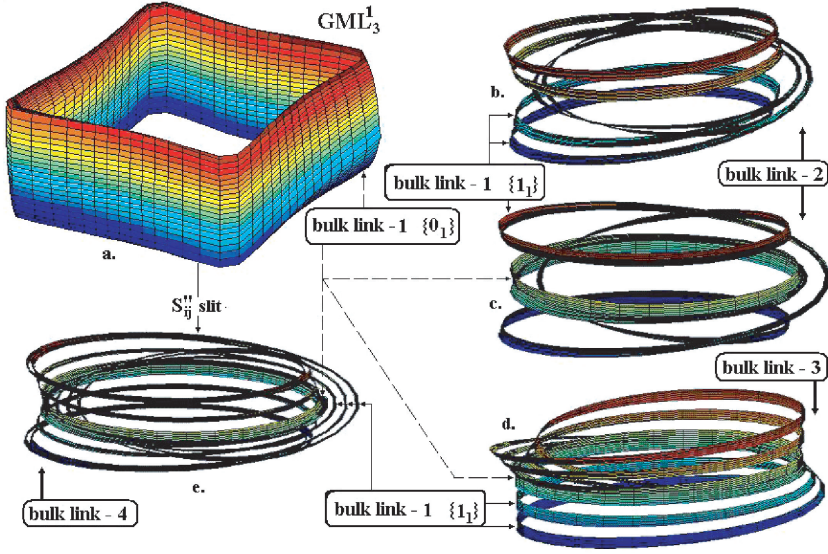
Figure 13

corresponding straight line on the plane figures in the radial cross section). Examples of shapes of the radial cross sections before and after the cutting process are given in the table of Fig. 12.

Similarly we may prove the following theorem

THEOREM 5. *If the number of twisting is $n \equiv 3\omega + 2$, where ω is an arbitrary integer number, and the GML_3^n body is cut along some of its slit-surfaces, then, similarly to the previous theorem, nine different cases hold:*

Case A. *after an* SVB-*zone-slit of the GML_3^n body, an object bulk link-2, of the $GML_3^{3(3(\omega+1)+1)}$ bodies appears, whose structure are bulk link-1 $\{(4\omega+3)_1\}$ and their radial cross sections are three angular mirror symmetric plane figures, i.e. for each natural $\omega = 0, 1, 2, \ldots$*

$$(32) \qquad GML_3^{3\omega+2} \rightarrow^{SVB} \text{link-2 of the two } GML_3^{9\omega+12};$$

Case B. *after an* SB-*zone-slit of the GML_3^n body, an object bulk link-2, of the $GML_3^{3(3(\omega+1)+1)}$ and $GML_4^{4(3(\omega+1)+1)}$ bodies appears, whose structure are link-1 $\{(4\omega+3)_1\}$ and their radial cross sections correspondingly are three and four angular plane figures, i.e. for each natural $\omega = 0, 1, 2, \ldots$*

$$(33) \qquad GML_3^{3\omega+2} \rightarrow^{SB} \text{link-2 of the } GML_3^{9\omega+12} \text{ and } GML_4^{12\omega+16};$$

Case C. *after an* SV-*zone-slit of the GML_3^n body, an object bulk link-3 appears. One component of this object is a bulk link-1 $\{0_1\}$ of the $GML_3^{3\omega+2}$ body, the*

second and third are bulk link-1 $(4\omega + 3)_1$ *(see Remark 5. C.) of the* $GML_3^{3(3(\omega+1)+1)}$ *and* $GML_4^{4(3(\omega+1)+1)}$ *bodies, whose radial cross sections correspondingly are three and four angular plane figures; i.e. for each natural* $\omega = 1, 2, \ldots$

$$\text{(34)} \qquad \begin{aligned} GML_3^{3\omega+2} \rightarrow^{SV} \text{ link-3 of the } GML_3^{3\omega+2}, \\ GML_3^{9\omega+12} \text{ and } GML_4^{12\omega+16}; \end{aligned}$$

Case D. *after an* SV_{ij}*-zone-slit of the* GML_3^n *body an object bulk link-2 appears. One component of this object is a bulk link-1* $\{0_1\}$ *of the* $GML_3^{3\omega+2}$ *body and the second is a bulk link-1* $\{(4\omega + 3)_1\}$ *of the* $GML_2^{2(3(\omega+1)+1)}$ *bodies, whose radial cross sections correspondingly are three and two angular plane figures; i.e. for each natural* $\omega = 1, 2, \ldots$

$$\text{(35)} \qquad GML_3^{3\omega+2} \rightarrow^{SV_{ij}} \text{ link-2 of the } GML_3^{3\omega+2} \text{ and } GML_2^{6\omega+8};$$

Case E1. *after an* S_{ij}^**-zone-slit of the* GML_3^n *body, an object bulk link-2 appears. One component of this object is a bulk link-1* $\{0_1\}$ *of the* $GML_6^{6\omega+4}$ *body and the second is a bulk link-1* $\{(4\omega + 3)_1\}$ *of the* $GML_3^{3(3(\omega+1)+1)}$ *body, whose radial cross sections correspondingly are six and three angular plane figures; i.e. for each natural* $\omega = 1, 2, \ldots$

$$\text{(36)} \qquad GML_3^{3\omega+2} \rightarrow^{S_{ij}^*} \text{ link-2 of the } GML_6^{6\omega+4} \text{ and } GML_3^{9\omega+12};$$

Case E2. *after an* $S_{ij}^\#$*-zone-slit of the* GML_3^n *body, an object bulk link-2 appears. One component of this object is a bulk link-1* $\{0_1\}$ *of the* $GML_3^{3\omega+2}$ *body and the second is a bulk link-1* $\{(4\omega + 3)_1\}$ *of the* $GML_3^{3(3(\omega+1)+1)}$ *body, whose radial cross sections correspondingly are six and three angular plane figures; i.e. for each natural* $\omega = 1, 2, \ldots$

$$\text{(37)} \qquad GML_3^{3\omega+2} \rightarrow^{S_{ij}^\#} \text{ link-2 of the } GML_3^{3\omega+2} \text{ and } GML_3^{9\omega+12};$$

Case E3. *after an* $S_{ij}^\flat$*-zone-slit of the* GML_3^n *body, an object bulk link-3 appears. One component of this object is a bulk link-1* $\{0_1\}$ *of the* $GML_3^{3\omega+2}$ *body and the second and third are a bulk link-1* $\{(4\omega + 3)_1\}$ *of the* $GML_3^{3(3(\omega+1)+1)}$ *and* $GML_5^{5(3(\omega+1)+1)}$ *bodies, whose radial cross sections correspondingly are three and five angular plane figures; i.e. for each natural* $\omega = 1, 2, \ldots$

$$\text{(38)} \qquad \begin{aligned} GML_3^{3\omega+2} \rightarrow^{S_{ij}^\flat} \text{ link-3 of the } GML_3^{3\omega+2}, \\ GML_3^{9\omega+12} \text{ and } GML_5^{15\omega+20}; \end{aligned}$$

Case E4. *after an* S_{ij}'*-zone-slit of the* GML_3^n *body, an object bulk link-3 appears. One component of this object is a bulk link-1* $\{0_1\}$ *of the* $GML_3^{3\omega+2}$ *body and the second and third are a bulk links-1* $\{(4\omega + 3)_1\}$ *of the* $GML_4^{4(3(\omega+1)+1)}$ *bodies,*

whose radial cross sections are four angular plane figures; i.e. for each natural $\omega = 1, 2, \ldots$

$$(39) \qquad \begin{array}{c} GML_3^{3\omega+2} \rightarrow^{S'_{ij}} \text{ link-3 of the } GML_3^{3\omega+2}, \\ GML_4^{12\omega+16} \text{ and } GML_4^{12\omega+16}; \end{array}$$

Case F. *after an S_{ii}-zone-slit (for any $i = 0, 1, 2$) of the GML_3^n body, an object bulk link-2 appears. One component of this object is a bulk link-1 $\{0_1\}$ of the $GML_9^{3(3\omega+2)}$ body and the second is a bulk link-1 $\{(4\omega + 3)_1\}$ of the $GML_2^{2(3(\omega+1)+1)}$ bodies; i.e. for each natural $\omega = 1, 2, \ldots$*

$$(40) \qquad GML_3^{3\omega+2} \rightarrow^{S_{ii}} \text{ link-2 of the } GML_9^{9\omega+6} \text{ and } GML_2^{6\omega+8};$$

In these nine cases only *three different* type of links appear (particular examples of the results of the Theorem 5. when $\omega = 1$ are shown in:

– Fig. 14.b., which corresponds to the cases A. and B.;
– Fig. 14.c., which corresponds to the cases D., E1., E2., F.;
– Fig. 14.d., which corresponds to the cases C., E3., E4.).

REMARK 7. 1. (Non-convex cases). *Separately, by recalling the Remark 3 and using the previous theorems, theoretically it is possible to prove similar results for the Generalized Möbius-Listing's Bodies GML_3^n, with* non-convex 3-*symmetric and*
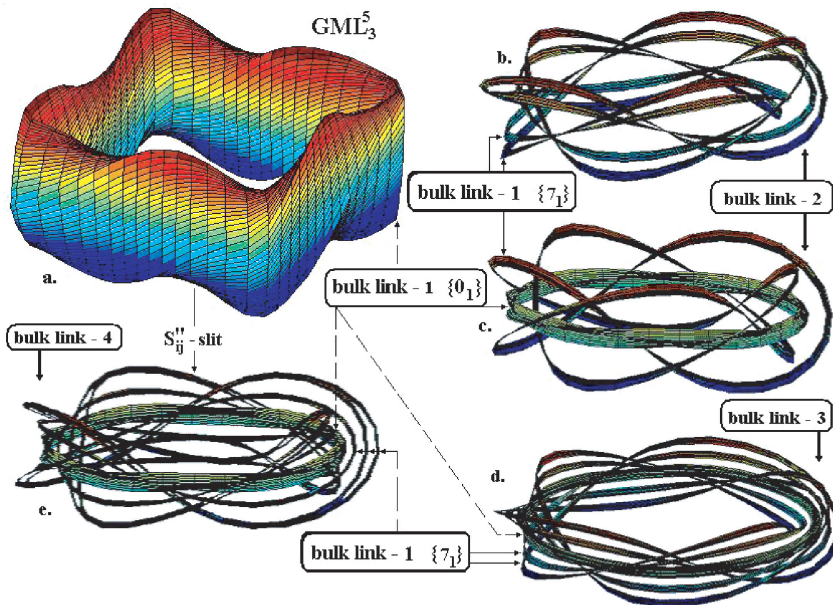

Figure 14

3-angular *radial cross sections, but it is necessary to specify each particular situation (since there exist a lot of different cases). We consider now only a particularly interesting case.*

Case E5. This case holds only if the radial cross section is a non-convex plane figure similar to that appearing in Fig. 15. In this case, after cutting, three or four different components appear.

S''_{ij}*-zone-slit—is a straight line tangent to the arc between the i and j sides of the* non-convex *planar figure of radial cross section of the body (see e.g. Fig. 15 or Fig. 16);*

Case E5.—for Theorem **3.** *after an S''_{ij}-zone-slit of the $GML_3^{3\omega}$ body, an object bulk link-3 $\{(3 \cdot 2\omega)_?^3\}$ of the GML_3^n bodies appears, whose structure are bulk links-1 0_1, and whose radial cross sections are three angular plane figures, i.e. for each natural $\omega = 0, 1, 2, \ldots$*

$$(41) \qquad GML_3^{3\omega} \to^{S_{ij}} link\text{-}3\{(6\omega)_?^3\} \text{ of the three } GML_3^{3\omega}.$$

An example of the shapes of the radial cross sections, before and after an S''_{ij}-zone-slit, is shown in Fig. 15, and a general view of the bulk link-3, when $\omega = 2$, is given in Fig. 11.c.;

Case E5.—for Theorem **4.** *after an S''_{ij}-zone-slit of the $GML_3^{3\omega+1}$ body, an object bulk link-4 appears. One component of this object is a bulk link-1 $\{0_1\}$ of the $GML_3^{3\omega+1}$ body, while the second, third and fourth components are bulk links-1 $\{(4\omega + 1)_1\}$ (see Remark 5. C.) of the two $GML_3^{3\cdot3(\omega+1)}$ and one $GML_4^{3\cdot4(\omega+1)}$ bodies, whose radial cross sections are three and four angular plane figures; i.e. for each natural $\omega = 1, 2, \ldots$*

$$(42) \qquad \begin{array}{l} GML_3^{3\omega+1} \to^{S''_{ij}} link\text{-}4 \text{ of the } GML_3^{3\omega+1}, \\ GML_4^{12\omega+12} \text{ and two } GML_3^{9\omega+9}. \end{array}$$

An example of the shapes of the radial cross sections, before and after an S''_{ij}-zone-slit, is shown in Fig. 16, and a general view of the bulk link-3, when $\omega = 0$, is given in Fig. 13.e.;

Case E5.—for Theorem **5.** *after an S''_{ij}-zone-slit of the $GML_3^{3\omega+2}$ body, an object bulk link-4 appears. One component of this object is a bulk link-1 $\{0_1\}$ of the*
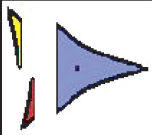
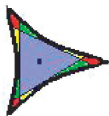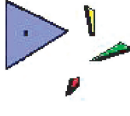| Shapes of radial cross section GML_3^n	- slit	Parameters of the objects which appear after cutting			
		Shapes of radial cross sections	if n=3ω	Link group of elements	Link group link-3
E5	S''_{ij}		link-3 of $GML_3^{3\omega}$ $GML_3^{3\omega}$ $GML_3^{3\omega}$	link-1 $\{0_1\}$	$\{(3 \cdot 2\omega)_?^3\}$

Figure 15

Shapes of radial cross section GML_3^n	– slit	Parameters of the objects which appear after cutting				
		Shapes of radial cross sections	if $n=3\omega+1$	Link group of elements	if $n=3\omega+2$	Link group of elements
E5	S_{ij}''		link-4 of $GML_3^{3\omega+1}$ $GML_3^{9\omega+9}$ $GML_3^{9\omega+9}$ $GML_4^{12\omega+12}$	link–1 $\{0_1\}$ $\{(4\omega+1)_1\}$ $\{(4\omega+1)_1\}$ $\{(4\omega+1)_1\}$	link- 4 of $GML_3^{3\omega+2}$ $GML_3^{9\omega+12}$ $GML_3^{9\omega+12}$ $GML_4^{12\omega+16}$	link–1 $\{0_1\}$ $\{(4\omega+3)_1\}$ $\{(4\omega+3)_1\}$ $\{(4\omega+3)_1\}$

Figure 16

$GML_3^{3\omega+1}$ *body, while the second, third and fourth components are bulk links-1* $\{(4\omega+3)_1\}$ *of the two* $GML_3^{3\cdot3((\omega+1)+1)}$ *and one* $GML_4^{3\cdot4((\omega+1)+1)}$ *bodies, whose radial cross sections are three and four angular plane figures; i.e. for each natural* $\omega = 1, 2, \ldots$

$$(43) \qquad GML_3^{3\omega+1} \to^{S_{ij}''} \text{link-4 of the } GML_3^{3\omega+1},$$
$$GML_4^{12\omega+16} \text{ and two } GML_3^{9\omega+12}.$$

An example of the shapes of the radial cross sections, before and after an S_{ij}''-zone-slit, is shown in Fig. 16, and a general view of the bulk link-3, when $\omega = 2$, is given in Fig. 14.e.

REMARK 8. Similarity and Difference. a.) *If $n = 3\omega$, then the structure of the bulk links, which appear after cutting the $GML_3^{3\omega}$ body, are similar to the ribbon links appearing after an s-zone slit of the $GML_3^{3\omega}$ surface (see Theorem 1 case A. and Theorem 3);*

b.) *If $n = 3\omega$, then, after cutting the $GML_3^{3\omega}$ body, never appears a bulk link analog to the ribbon link appearing after a b-zone slit of the $GML_3^{3\omega}$ surface (see Theorem 2. case A.);*

c.) *If $n = 3\omega + 1$, then the bulk link-1 $(4\omega + 1)_1$ appearing after cutting the $GML_3^{3\omega+1}$ body, is similar to the ribbon links-1 which appear after an s-zone slit of the $GML_3^{3\omega+1}$ surface (see Theorem 1 case B. and Theorem 4);*

d.) *If $n = 3\omega + 2$, then the bulk link-1 $(4\omega + 3)_1$ appearing after cutting the $GML_3^{3\omega+2}$ body, is similar to the ribbon links-1 which appear after an s-zone slit of the $GML_3^{3\omega+2}$ surface (see Theorem 1 case C. and Theorem 5);*

e.) *for arbitrary n, after cutting the GML_3^n surface, never appears a ribbon link with three components (similarly to cases C., E3. and E4. of the Theorems 4 or 5).*

REMARK 9. a.) *Each results of the the previous Theorems still hold when the basic line is a closed space line, but the link structure of the geometric objects, appearing after cutting, is completely different;*

b.) *The structure of the ribbon links, appearing after k-times cutting along arbitrary s-lines of a GML_2^n surface with radial cross section consisting in a simple star, has been studied in* [17]*;*

c.) *The structure of the ribbon links, appearing after k-times cutting along arbitrary s-lines of a GML_m^n surface whose radial cross section is an m-symmetric star-like ''line'', has been studied in* [18], [19];

d.) *The structure of the bulky links, appearing after cutting along the corresponding slit-surfaces of GML_2^n bodies, has been studied in* [7];

e.) *The structure of the bulky links, appearing after k-times cutting along the corresponding slit-surfaces of GML_2^n bodies, is at present unknown.*

REFERENCES

[1] D. CARATELLI - P. NATALINI - P. E. RICCI - J. GIELIS - I. TAVKHELIDZE, *The Robin problem for Helmholtz equation in a starlike planar domain*, Georgian Math. J. 18, (2011), 465–479. DOI 10.1515/GMJ.2011.0031.

[2] D. CARATELLI - P. E. RICCI - J. GIELIS, *The Robin problem for the Laplace equation in a three-dimensional starlike domain*, Appl. Math. Comput., 218 (3), (2011), 713–719.

[3] C. CASSISA - I. TAVKHELIDZE, *About Some Geometric characteristic of the Generalized Möbius Listing's urfaces*, Georgian Electro. Sci. J.: Comp. Sci. Telecom., Tbilisi, No. 4 (21), (2009), 54–84.

[4] H. DOLL - J. HOSTE, *A Tabulation of Oriented Links*, Math. Comput., 57, (1991), 747–761.

[5] Y. FOUGEROLLE - A. GRIBOK - S. FOUFOU - F. TRUCHETET - M. A. ABIDI, *Radial Supershapes for Solid Modeling*, J. Comput. Sci. Tech., Mar. (2006), vol. 21, No. 2, 238–243.

[6] J. GIELIS - D. CARATELLI - Y. FOUGEROLLE - P. E. RICCI - T. GERATS, *Universal Natural Shapes from Unifying Shape Description to simple Methods for Shape Analysis and Boundary Value Problems*, PLoSONE-D-11-01115R2 10.1371/journal.pone.0029324.

[7] J. GIELIS - P. E. RICCI - I. TAVKHELIDZE, *About ''Bulky'' Links generated by Generalized Möbius-Listing bodies GML_2^n*, (submitted).

[8] A. GRAY - E. ABBENA - S. SALAMON, *Modern Differential Geometry of Curves and Surfaces with Mathematica*, (Third Edition), Stud. Adv. Math., Chapman & Hall/CRC, Boca Raton, FL, 2006.

[9] G. KUPENBERG, *Quadrisecants of Knots and Links*, J. Knot Theory Ramifications, 3, (1994), 41–50.

[10] C. LIVINGSTON, *Knot Theory*, The Carus Mathematical Monographs, vol. 24, The Math. Assoc. America, 1993, 1–255.

[11] T. OHTSUKI, *Quantum Invariants a Study of Knots,* 3-*Manifolds and Their Sets*, Ser. Knots Everything, vol. 29, (2002), 1–508.

[12] P. E. RICCI - I. TAVKHELIDZE, *About Some Geometric Characteristic of the Generalized Möbius Listing's surfaces*, Georgian Math. J., vol. 18, (2009), N. 2.

[13] A. SOSSINSKY, *Knots Mathematics with a Twist*, Harvard Univ. Press, 2002, 1–147.

[14] I. TAVKHELIDZE, *On the some properties of one class of geometrical figures and lines*, Rep. Enlarged Sess. Semin. I. Vekua Appl. Math., vol. 16, N. 1, (2001), 35–38.

[15] I. TAVKHELIDZE - P. E. RICCI, *Classification of a wide set of Geometric figures, surfaces and lines (Trajectories)*, Rend. Accad. Naz. Sci. XL Mem. Mat. Appl., 124°, vol. XXX, fasc. 1, (2006), 191–212.

[16] I. TAVKHELIDZE, *Classification of a Wide Set of Geometric Figures*, Lect. Notes TICMI, Tbilisi, vol. 8, (2007), 53–61.

[17] I. TAVKHELIDZE - C. CASSISA - P. E. RICCI, *About Connection of the generalized Möbius Listing's surfaces with Sets of Knots and Links*, Lect. Notes Semin. Interdiscip. Mat., vol. 9, (2010), 187–200.

[18] I. TAVKHELIDZE, *About Connection of the Generalized Möbius Listing's surfaces GML_m^n with Sets of Ribbon Knots and Links*, Proc. Intern. Conf. "Modern Algebra and its Applications"—Batumi, Georgia, 2010 (20–26 IX), 147–152.

[19] I. TAVKHELIDZE, *About Connection of the Generalized Möbius Listing's surfaces with Sets of Ribbon Knots and Links*, Proc. Ukrainian Math. Congr. S. 2, Topology and geometry—Kiev, 2011, 117–129.

[20] E. W. WEISSTEIN, *The CRC concise Encyclopedia of Mathematics*, (Second edition), Chapman & Hall/CRC, Boca Raton, FL, (2003).

I. Tavkhelidze
Iv. Javakhishvili Tbilisi State University
Department of Mathematics University
Street 2, Tbilisi 0186, Georgia
ilia.tavkhelidze@tsu.ge

C. Cassisa
Università di Roma "La Sapienza"
Dipartimento di Matematica
P.le A. Moro, 2, 00185 Roma
Italia
cassisa@mat.uniroma1.it

J. Gielis
University of Antwerp
Department of Bioscience Engineering 2020 Antwerp
Belgium
johan.gielis@ua.ac.be

P. E. Ricci
Università Campus Bio-medico di Roma
Via Alvaro del Portillo
21 00128 Roma (Italia)
paoloemilioricci@gmail.com